Advanced computation of enthalpies for a range of hydroformylation reactions with a predictive power to match experiments

Tamara Papp[a], Péter R. Nagy[c,d,e,*], Tamás Kégl[a,b,*]

[a] *Department of Inorganic Chemistry, University of Pécs, Ifjúság útja 6., H-7624 Hungary and János Szentágothai Research Center, Pécs, Ifjúság útja 34., H-7624 Hungary*
[b] *MTA-PTE Research Group for Selective Chemical Syntheses*
[c] *Department of Physical Chemistry and Materials Science, Faculty of Chemical Technology and Biotechnology, Budapest University of Technology and Economics, Műegyetem rkp. 3., H-1111 Budapest, Hungary*
[d] *HUN-REN-BME Quantum Chemistry Research Group, Műegyetem rkp. 3., H-1111 Budapest, Hungary*
[e] *MTA-BME Lendület Quantum Chemistry Research Group, Műgyetem rkp. 3., H-1111 Budapest, Hungary*

Abstract

While hydroformylation is a central homogeneous catalytic industrial processes, we find a relatively large (17 kcal/mol) scatter of DFT reaction enthalpies with a range of widely-employed DFT methods, unexpected in organic chemistry. Thus, we obtained gold standard hydroformylation enthalpies for a large variety of substrates exploiting the local natural orbital method. The corresponding hydroformylation enthalpies of ethylene and propylene agree with the experiments within a few tenth of a kcal/mol. This predictive power enabled the study of nuanced trends in the hydroformylation for a wide range of aliphatic and aromatic substrates as a function of chain elongation, branching, and substituent effects.

Keywords: enthalpy, hydroformylation, density functional theory, coupled cluster theory

1. Introduction

Hydroformylation, also known as oxo synthesis, is the formal addition of CO and H_2 to the C=C double bond of alkenes in the presence of metal-based catalyst to form aldehydes (Figure 1). Hydroformylation is considered one of the largest homogeneous catalytic industrial processes [1] as the resulting aldehydes can be easily converted into several secondary products. As a consequence, this reaction has been described in a vast number of comprehensive reviews. [2–5] The most popular hydroformylation catalysts are Co [6] and Rh [7, 8] based systems, in combination with a wide variety of phospines, although several other Pt, [9] Ru [10, 11], Ir [12] and in some cases Fe [13] based catalysts have also been reported. With platinum catalysts, high enantioselectivities were achieved in some cases, however the activity and regioselectivity of the Pt-based catalysts are usually lower than those of the rhodium-containing systems. It is important to note that Pt-catalysts are inactive in hydroformylation without co-catalyst. In this role, tin(II) chloride is employed in the majority of cases [14, 15], however, tin(II) fluoride can result in active catalysts as well, especially when higher temperature is required. [16]

The generally accepted catalytic cycle, introduced by Heck and Breslow [17], consists of the following elementary steps: alkene coordination to the metal complex, its insertion into the metal-H bond, CO activation and its insertion into metal-alkyl bond, and finally the product forming step, the dihydrogen activation and aldehyde elimination. The last step of the catalytic cycle is always exergonic.

Nowadays not only experimental but also computational chemistry plays an increasingly important role in the investigation of reaction mechanisms and the factors influ-

*Corresponding author
Email addresses: nagy.peter@vbk.bme.hu (Péter R. Nagy), tkegl@gamma.ttk.pte.hu (Tamás Kégl)

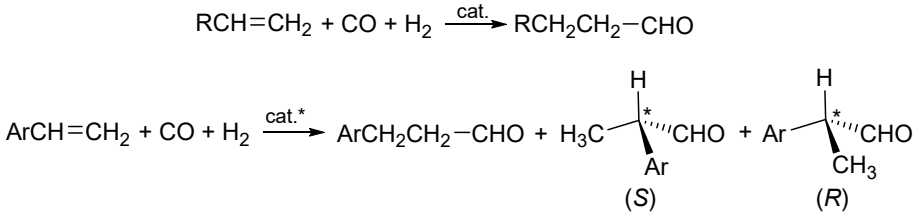

Figure 1: General equation for the hydroformylation of aliphatic ethylene derivatives (top) and various prochiral vinyl aromatics (bottom).

encing the outcome of catalytic reactions. [18] The reaction mechanism of $HCo(CO)_3$-catalyzed hydroformylation of propene has been systematically studied, and they found that the olefin insertion process is reversible, in agreement with the experiments. [19]

The platinum-catalyzed hydroformylation of propene has been also investigated with density functional theory. [20] It has been found that the olefin insertion step influences the regioselectivity, furthermore the calculated ratio of the linear regioisomer is very similar to the experimental value. Modeling the Pt-catalyzed asymmetric hydroformylation of styrene revealed that the enantioselectivity is also determined during the olefin insertion step when the chiraphos ligand is utilized as chiral ligand.[21] The hydroformylation of ethylene employing $HRh(PH_3)_2(CO)$ catalyst has been studied by Cundari and Decker. They calculated the enthalpy of the reaction at B3LYP level, and it was overestimated by about 7 kcal/mol. In contrast, the CCSD(T) methodology more accurately estimated the experimental results. [22]

Therefore, here we extend these comparisons to a wide-range of hydroformylation reactions studying a variety of substrates including chain elongation, branching, and substituent effects. To that end, first, we benchmark a representative set of popular DFT methods against gold standard CCSD(T) references, and when available, experiments and suggest a reliable and efficient DFT method for hydroformylation reactions.

2. Computational Details

The geometry optimization were computed with the B97-D3 functional. The list and references corresponding to all other tested DFT methods can be found in the Supporting Information. [23] We used the valence triple-ζ def2-TZVP basis set for all atoms in the DFT computations. [24] The reference CCSD(T) computations were accelerated with the local natural orbital (LNO)[25–29] method as implemented in the Mrcc quantum chemistry program suite [30, 31] and detailed in Section 3.

3. CCSD(T) reference computations

The efficiency of the LNO-CCSD(T) approach [25–28] allowed us to reach the complete basis set (CBS) limit of the reaction energies via basis set extrapolation [32] using the extensive aug-cc-pVXZ (X=T,Q) basis sets. [33] To study various aliphatic and aromatic substrates and corresponding chain elongation, branching, and substituent effects, a total of about 60 different molecules were modeled containing up to 29 atoms. Without the LNO approach, even one of such large-scale computations at the CBS(T,Q) quality would be at the very limit of highly-optimized and parallel conventional CCSD(T) implementations.[34] Compared to that the LNO approach was shown to consistently provide outstanding accuracy in comparison to both conventional CCSD(T) and alternative local correlation approaches for various chemical applications,[27] as reviewed recently in Ref. 29. Moreover, the Normal and Tight settings of the LNO approximations were employed to extrapolate toward the local approximation free (LAF)

CCSD(T) limit, [27, 29] yielding the Normal–Tight (N–T) extrapolated LNO-CCSD(T) energies of

$$E^{\mathrm{N-T}} = E^{\mathrm{Tight}} + (E^{\mathrm{Tight}} - E^{\mathrm{Normal}})/2. \qquad (1)$$

The step size between the Normal and Tight settings can also be used as an error estimate [$\pm(E^{\mathrm{Tight}} - E^{\mathrm{Normal}})/2$] for the remaining uncertainty of the LNO approximation. Furthermore, we compute a basis set incompleteness (BSI) estimate using the third of the difference between the aug-cc-pVQZ and the CBS(T,Q) results. By combining the BSI and LNO error estimates, we find that the employed N–T extrapolated LNO-CCSD(T)/CBS(T,Q) reaction energies exhibit lower than ±0.1 kcal/mol uncertainty, except with the OH and OMe substituents, where ±0.15 and ±0.12 kcal/mol were found, respectively. For the reactions with alkene reactants, the even better Tight–very Tight (T–vT) LAF extrapolated LNO settings [27, 29] are obtained, pushing all corresponding convergence measures below ±0.1 kcal/mol. Finally, to estimate the BSI at the CBS(T,Q) level, with the ethene reactant, we find the CBS(T,Q) and CBS(Q,5) results with aug-cc-pVXZ (X=T,Q,5) bases in agreement within 0.02 kcal/mol, indicating outstanding basis set convergence already at the CBS(T,Q) level. The benefit of staying at the N–T LAF extrapolated LNO-CCSD(T)/CBS(T,Q) level is that even the most demanding Tight LNO-CCSD(T)/aug-cc-pVQZ computation took for the largest studied molecule ca. 8 hours and 4 GB memory using 7 processor cores. While this is still 1–2 order of magnitude higher cost than for hybrid DFT energies, it is comparable to DFT structure optimization and harmonic frequency evaluation.

It is worth briefly noting about the more general significance of such well-converged and affordable reference CCSD(T) computations. At the first stage of benchmark studies enabled already by the earlier versions of local correlation based CCSD(T) methods, researchers could target a set of larger molecules beyond the limits of conventional CCSD(T), with acceptable approximations to the true CCSD(T)/CBS result. The resulting references were successfully used by multiple groups to, e.g., report statistical analysis on the accuracy of lower-cost approaches, such as DFT, across a variety of chemical applications.[35–43] Besides these more general benchmark compilations, early adopter groups also started to employ local CCSD(T) benchmarks in computational studies targeting specific questions, as reviewed recently.[29] The present study represents the next stage of this progression, enabled by the decreased computational requirements resulting from continuous advances in local CCSD(T) approaches. Specifically here, all electronic energies and hence enthalpies could be relatively routinely evaluated at the LNO-CCSD(T)/CBS(T,Q) level, yielding uncertainty estimates at the 0.1–0.2 kcal/mol level. Therefore, this study demonstrates that one can now affordably overcome DFT uncertainties and take advantage of the higher predictive power of CCSD(T), even with the straightforward approach of replacing DFT energies for all computed species. While such high level of caution is probably not needed for all applications, this is a very robust and easily automatable solution that has utility especially at the age of data-driven approaches.

4. Results and Discussion

For the selection of an accurate functional, in terms of reproduction of experimental geometries, a variety of DFT functionals were tested belonging to the pure GGA, hybrid, meta-GGA, meta-hybrid-GGA, range-separated hybrid, and double hybrid categories. The bond distances between heavy atoms of the substrate ethylene and the product propanal molecules were selected as reference data. The carbon-carbon distance in ethylene was a subject of numerous investigations. The benchmark value for this paper was taken from the work of Craig et al.[44] where a semi-experimental approach was used with adjusting the rotational constants obtained from rotational spectroscopy by vibration-rotation constants calculated from the results

Table 1: The C-C and C-O bond distances (in Å) of ethylene[a] and propanal[b] molecules at various levels of theory as well as the mean absolute deviation of the geometrical data. All distances are given in Å.

Method	C1-C2[a]	C1-C2[b]	C2-C3[b]	C3-O[b]	MAD
B3LYP	1.324	1.523	1.505	1.204	0.005
CAM-B3LYP	1.319	1.516	1.499	1.200	0.010
B98	1.326	1.525	1.510	1.203	0.004
BLYP-D3	1.333	1.532	1.516	1.216	0.006
B97-D	1.332	1.530	1.514	1.210	0.003
B97-D3	1.331	1.525	1.510	1.210	0.001
ωB97X-D	1.321	1.518	1.503	1.200	0.008
ωB97X-D4	1.325	1.521	1.507	1.203	0.005
BP86	1.333	1.526	1.511	1.215	0.003
M06-2X	1.321	1.518	1.503	1.200	0.008
MN12-SX	1.320	1.514	1.503	1.197	0.011
MN12-L	1.321	1.511	1.498	1.202	0.010
M06-L	1.320	1.514	1.502	1.195	0.012
PBE	1.332	1.523	1.508	1.214	0.001
PBE0	1.323	1.514	1.499	1.201	0.009
TPSS	1.330	1.527	1.511	1.214	0.001
BMK	1.325	1.530	1.515	1.197	0.007
BMK-D3	1.332	1.529	1.515	1.197	0.007
MP2	1.332	1.518	1.502	1.214	0.005
B2PLYP	1.327	1.520	1.505	1.208	0.005
B2PLYP-D3	1.327	1.520	1.504	1.208	0.005
exp.	1.332	1.523	1.509	1.210	–

of quantum chemical calculations. For propanal, the structural data reported by Kuchitsu were used as reference.[45] Most functionals resulted in satisfactory agreement with the experimental data (Table 1). Among them, the B97-D3 functional was selected for obtaining geometries and enthalpy corrections throughout this study.

Since no direct experimental thermochemistry data are available for the hydroformylation reactions, the reaction enthalpy was obtained from the experimental heat of formation data of H_2, CO, ethylene, propylene, propanal, and n-butanal. With this approach, the experimental value of the enthalpy of the hydroformylation of ethylene was calculated to be −31.21 kcal/mol and −30.58 kcal/mol, for using the enthalpy of formation values of propanal reported by Connett [46], and Wiberg et al. [47], respectively.

The computed data for the enthalpy of hydroformylation of ethylene at several levels of theory are summarized in Table 2. There are numerous models that provided good to excellent agreement with the experimental data, such as the LNO-CCSD(T) and MP4 levels of theory. Regarding the DFT methods, the results span the surprisingly wide range of [−26.64,−43.23], that is a 17 kcal/mol interval, at least for reaction enthalpies of relatively simple, closed-shell organic molecules. In general, the lack of clear consensus even among the more advanced and popular hybrid methods hinders one to follow best-practice DFT model selection approaches and makes the selection from the large number of DFT methods complicated. After taking advantage of reliable references, the B97-D3 functional can be emphasized for its accuracy, but the BLYP-D3, B3LYP, and the double hybrid B2PLYP methods provided good agreement as well. The MN12-SX (−31.27 kcal/mol) and the local MN12-L (−31.73 kcal/mol) Minnesota functionals developed by Truhlar and co-workers were also shown to be accurate. MN12-SX is a screened-exchange (SX) hybrid functional with 25% HF exchange in the short-range and 0% exact exchange in the long-range. The other Minnesota functionals examined here (M06, M06-2X hybrid and M06-L local functional) gave more significant deviations from the experimental result. In general, the hybrid functionals, with the exception of B97 and B3LYP, did not give satisfying estimations of the enthalpy of hydroformylation. By examining certain functionals with and without D3 dispersion correction, the correction does not improve the accuracy (e.g., for PBE, OLYP, B2PLYP, BMK), expect for BLYP, which indicates the presence of additional significant sources of errors besides the description of dispersion. Regarding the perturbative wave function methods, MP2 overestimates, while the inclusion of triple excitations in the fourth order Møller-Plesset method did not bring noticeable change in the reaction enthalpy. In light of the CCSD(T) data, this highlights the importance of the higher-order correlation of the single and double excitations as included in CC but missing from the MP methods.

Selecting the B97-D3 and LNO-CCSD(T) levels of theory, the enthalpy of hydroformylation of various other olefins were calculated (Table 3). From the enthalpies of formation, the enthalpy of propylene hydroformylation towards n-butanal is found to be −27.31 kcal/mol, whereas no experimental enthalpy of formation can be obtained for isobutanal. Both levels resulted in reasonable agreements with the experimental value. In general, B97-D3 tends to underestimate the ΔH values by approximately 1.5 kcal/mol in comparison to the coupled cluster method. It can also be concluded, that the branched aldehydes are thermodynamically more stable as compared to the linear aldehydes and the results saturate with the increase of the chain length.

The enthalpies of styrene and para-substituted styrene derivatives were also calculated at B97-D3 level of theory and with the LNO-CCSD(T) method (Table 4 and Figures S1 and S2 in the Supporting Information). Here, we find both for linear and branched aldehyde isomers the expected saturation of the thermodynamical stability upon

Table 2: The calculated enthalpies of hydroformylation of ethylene at various levels of theory.

Method	ΔH [kcal/mol]	Method	ΔH [kcal/mol]
PBE	−40.92	BMK	−34.53
PBE-D3	−42.85	BMK-D3	−36.49
revPBE-D3	−35.41	BP86	−36.06
PBE0	−43.23	BP86-D3	−38.93
B98	−37.87	M06	−36.46
OLYP	−29.33	M06-L	−39.65
OLYP-D3	−38.59	M06-2X	−34.25
O3LYP	−41.85	MN12-L	−31.73
BLYP	−26.64	MN12-SX	−31.27
BLYP-D3	−30.57	mPWPW	−37.76
B2PLYP	−31.34	mPW1PW	−40.66
B2PLYP-D3	−32.79	TPSSh	−34.72
B3LYP	−31.34	TPSS	−33.08
CAM-B3LYP	−35.61	MP2 [48]	−33.16
B97-D	−29.97	MP4(SDQ) [49]	−30.83
B97-D3	−31.85	MP4(SDTQ) [50]	−30.28
ωB97X-D	−37.71	LNO-CCSD(T) [27]	−31.14
ωB97X-D4	−36.45		

Table 3: Enthalpy of hydroformylation [in kcal/mol] of various olefins at B97-D3 and LNO-CCSD(T) level of theory.

Olefin	ΔH^a_{linear}	ΔH^b_{linear}	$\Delta H^a_{branched}$	$\Delta H^b_{branched}$
Propylene	−26.81	−28.19	−27.24	n.a.
1-Butylene	−28.45	−29.99	−28.91	−30.62
1-Pentene	−28.30	−29.85	−28.89	−30.53
Cyclopentene	−25.00	−26.56	n.a.	n.a.
1-Hexene	−27.07	−28.57	−27.65	−29.88
1-Heptene	−27.11	−28.61	−27.73	−29.31
1-Octene	−27.02	−28.55	−27.61	−29.24

[a] at B97-D3 level of theory; [b] with LNO-CCSD(T)

Table 4: Enthalpy of hydroformylation and hydrogenation [in kcal/mol] of styrene and para-substituted styrene derivatives at B97-D3 and LNO-CCSD(T) level of theory.

	hydroformylation				hydrogenation	
Substituent	ΔH^a_{linear}	ΔH^b_{linear}	$\Delta H^a_{branched}$	$\Delta H^b_{branched}$	ΔH^a	ΔH^b
H	−24.75	−26.89	−24.61	−26.44	−22.70	−27.81
Ac	−24.64	−26.90	−24.14	−26.12	−22.93	−28.10
CF_3	−24.82	−26.96	−24.31	−26.13	−23.19	−28.25
Cl	−24.56	−26.84	−24.32	−26.19	−22.74	−27.95
F	−24.53	−26.73	−24.39	−26.22	−22.62	−27.82
iPr	−24.59	−26.80	−24.66	−26.54	−22.44	−27.59
Me	−24.59	−26.79	−24.64	−26.48	−22.47	−27.65
OMe	−24.07	−26.56	−24.34	−26.40	−21.95	−27.44
NH_2	−23.78	−26.37	−24.36	−26.40	−21.46	−27.15
NMe_2	−23.69	−26.41	−24.41	−26.40	−21.24	−26.98
NO_2	−24.63	−26.92	−23.88	−25.85	−23.24	−28.37
OH	−24.16	−26.66	−24.33	−26.35	−22.05	−27.51
CN	−24.60	−26.96	−23.94	−25.94	−23.17	−28.38
COOH	−24.68	−26.93	−24.19	−26.18	−22.99	−28.19

[a] at B97-D3 level of theory; [b] with LNO-CCSD(T)

increasing the system size with an about 0.6–0.7 kcal/mol higher stability for the branched systems. The tendency of underestimating the reaction enthalpy by 2–3 kcal/mol is prominent for the B97-D3 functional, while the relative trends are recovered better. All in all, the investigated energy differences are very small compared to the DFT uncertainty, which highlights the importance of converging LNO-CCSD(T) with about a tenth of a kcal/mol error bars to study such nuances.

The *para*-substituent effects for the vinylaromatic substrate also span a small range of 0.6–0.7 kcal/mol at the LNO-CCSD(T) level, which range is overestimated almost by a factor of 2 by B97-D3. For instance, in the presence of the most electron donating (dimethylamino group with Hammett $\sigma_p = -0.81$) and the most electron withdrawing (nitro group with Hammett $\sigma_p = 0.8$) substituents the reaction enthalpy difference is approximately 0.5 kcal/mol for both the linear and branched pathways. Inspecting the relation of the Hammett constants and the reaction enthalpies in Figures S1 and S2 we find considerably better correlation at the LNO-CCSD(T) level. Since the DFT errors are lower for small (absolute) Hammett constants below 0.2 and are up to 20% higher with for groups with very strong electron donating/withdrawing properties, this non-systematic DFT error considerably weakens the correlation of Hammett constants and the reaction enthalpies.

While the focus of this work is hydroformylation, it is worthwhile to make a brief comparison to the analogous hydrogenation reactions. To that end the hydrogenation enthalpies for the same vinylaromatic substrates are collected in right part of Table 4. While the reaction enthalpies are fairly similar to the corresponding hydroformylation processes, by looking more closely at the LNO-CCSD(T) results, we can observe underlying differences. First, the B97-D3 errors are about twice as large as for hydrogenation than for hydroformylation. Second, the decomposition of LNO-CCSD(T) reaction energies show about 70% mean-field and 30% correlation energy contribution for hydroformylation, in contrast to the ca. 1% correlation contribution for hydrogenation. The latter can be explained by the small electron correlation effect between the two electrons in H_2, which plays a relatively larger role in hydrogenation than in hydroformylation. Nevertheless, this different physics behind the similar total reaction enthalpy values are not as well described by DFT, again highlighting the benefits of having LNO-CCSD(T) references.

The somewhat simpler hydrogenation reactions also enable to better understand the relation between the Hammett constants and reaction enthalpies (Figure S3). For hydrogenation, we find much more straightforward correlation between the Hammett constants and reaction enthalpies in the range of r^2=0.94–0.98 with both B97-D3 and LNO-CCSD(T). Moreover, the relation is inverted compared to case of hydroformylation (cf. Figures S1 and S2). Namely, as expected, electron withdrawing/donating groups stabilize/destabilize the *para*-substituted product of hydrogenation. In light of this, the effect of the additional carbonyl group in the hydroformylation product can be interpreted as competitive with electron withdrawing and synergistic with electron donating substituents. The somewhat larger strength of this effect compared to that of the *para*-substituent is consistent with the closer vicinity of the carbonyl group to the saturated bond as well as with the narrowing of the reaction enthalpy interval from hydrogenation to hydroformylation.

5. Conclusion

In this Letter, the theoretical estimation of the enthalpy of the industrially significant hydroformylation reaction has been discussed. It can be concluded that the molecular geometries were accurately reproduced by the B97-D3 functional. The LNO-CCSD(T) method gave excellent agreement for the reaction enthalpies in the cases where experimental heat of formation data were available. For the

rest of the substrates, the reaction enthalpies showed substantial uncertainties scattered in a 17 kcal/mol wide range with a number of popular DFT methods, but some, including B97-D3 showed fairly close agreement with the coupled cluster data. However, a systematic underestimation of the reaction enthalpies and a weakening of some qualitative trends could be observed at the DFT level when we studied the chain elongation, branching, and substituent effects on various aliphatic and aromatic substrates. This DFT uncertainties could be overcome by the ability to use highly converged LNO-CCSD(T) for all species studied here, demonstrating that efficient local CCSD(T) approaches now enable routine access to chemical accuracy even for all (medium-sized) species of an entire computational study.

6. Acknowledgment

This paper is dedicated to Professor Jan M. L. Martin on the happy occasion of his 60th birthday to recognize his outstanding contributions to computational chemistry. The authors gratefully acknowledge supported by the ÚNKP-22-4-I-PTE-1490 New National Excellence Program of Ministry for Innovation and Technology; the National Research, Development, and Innovation Office (Grant No. FK142489); ERC Starting Grant No. 101076972; and the János Bolyai Research Scholarship of the Hungarian Academy of Sciences; University of Pécs, project number 014_2023_PTE_RK/14. We acknowledge the Hungarian Governmental Information-Technology Development Agency for awarding this project access to the Komondor and the LEONARDO supercomputer, owned by the EuroHPC Joint Undertaking, hosted by CINECA (Italy) and the LEONARDO consortium.

7. Appendix A. Supplementary material

Tables containing the internal energies and Cartesian coordinates of each species appearing in this study, as well as computed data for the electronic structure calculations.

8. References

[1] K.-D. Wiese, D. Obst, M. Beller (2006).
[2] M. Orchin, W. Rupilius, Catalysis Reviews 6 (1972) 85–131.
[3] R. Franke, D. Selent, A. Boerner, Chem. Rev. 112 (2012) 5675–5732.
[4] F. Agbossou, J.-F. Carpentier, A. Mortreux, Chem. Rev. 95 (1995) 2485–2506.
[5] J. Pospech, I. Fleischer, R. Franke, S. Buchholz, M. Beller, Angew. Chem., Int. Ed. 52 (2013) 2852–2872.
[6] F. Hebrard, P. Kalck, Chem. Rev. 109 (2009) 4272–4282.
[7] M. Diéguez, O. Pàmies, C. Claver, Tetrahedron: Asymmetry 15 (2004) 2113–2122.
[8] G. T. Whiteker, C. J. Cobley, Top. Organomet. Chem. 42 (2012) 35–46.
[9] R. van Duren, J. I. van der Vlugt, H. Kooijman, A. L. Spek, D. Vogt, Dalton Trans. (2007) 1053–1059.
[10] L. Wu, I. Fleischer, R. Jackstell, I. Profir, R. Franke, M. Beller, J. Am. Chem. Soc. 135 (2013) 14306–14312.
[11] K. Tominaga, Y. Sasaki, J. Mol. Catal. A: Chem. 220 (2004) 159–165.
[12] I. Piras, R. Jennerjahn, R. Jackstell, A. Spannenberg, R. Franke, M. Beller, Angew. Chem., Int. Ed. 50 (2011) 280–284.
[13] S. Pandey, K. V. Raj, D. R. Shinde, K. Vanka, V. Kashyap, S. Kurungot, C. Vinod, S. H. Chikkali, J. Am. Chem. Soc. 140 (2018) 4430–4439.
[14] C. Y. Hsu, M. Orchin, J. Am. Chem. Soc. 97 (1975) 3553–3553.
[15] I. Schwager, J. Knifton, J. Catal. 45 (1976) 256–267.
[16] L. Kollár, T. Kégl, J. Bakos, J. Organomet. Chem. 453 (1993) 155–158.
[17] R. F. Heck, D. S. Breslow, J. Am. Chem. Soc. 83 (1961) 4023–4027.
[18] T. Kégl, RSC Advances 5 (2015) 4304–4327.
[19] C.-F. Huo, Y.-W. Li, M. Beller, H. Jiao, Organometallics 22 (2003) 4665–4677.
[20] A. Bedekovits, L. Kollár, T. Kégl, Inorg. Chim. Acta 363 (2010) 2029–2045.
[21] T. Papp, L. Kollár, T. Kégl, Organometallics 32 (2013) 3640–3650.
[22] S. A. Decker, T. R. Cundari, Organometallics 20 (2001) 2827–2841.
[23] S. Grimme, S. Ehrlich, L. Goerigk, J. Comput. Chem. 32 (2011) 1456–1465.
[24] F. Weigend, R. Ahlrichs, Phys. Chem. Chem. Phys. 7 (2005) 3297–3305.
[25] P. R. Nagy, M. Kállay, J. Chem. Phys. 146 (2017) 214106.
[26] P. R. Nagy, G. Samu, M. Kállay, J. Chem. Theory Comput. 14

(2018) 4193.

[27] P. R. Nagy, M. Kállay, J. Chem. Theory Comput. 15 (2019) 5275.

[28] P. B. Szabó, J. Csóka, M. Kállay, P. R. Nagy, J. Chem. Theory Comput. 19 (2023) 8166.

[29] P. R. Nagy, Chem. Sci. 15 (2024) 14556.

[30] M. Kállay, P. R. Nagy, D. Mester, L. Gyevi-Nagy, J. Csóka, P. B. Szabó, Z. Rolik, G. Samu, J. Csontos, B. Hégely, Á. Ganyecz, I. Ladjánszki, L. Szegedy, B. Ladóczki, K. Petrov, M. Farkas, P. D. Mezei, R. A. Horváth, MRCC, a quantum chemical program suite. See https://www.mrcc.hu/ (Accessed May 1, 2024).

[31] M. Kállay, P. R. Nagy, D. Mester, Z. Rolik, G. Samu, J. Csontos, J. Csóka, P. B. Szabó, L. Gyevi-Nagy, B. Hégely, I. Ladjánszki, L. Szegedy, B. Ladóczki, K. Petrov, M. Farkas, P. D. Mezei, Á. Ganyecz, J. Chem. Phys. 152 (2020) 074107.

[32] T. Helgaker, W. Klopper, H. Koch, J. Noga, J. Chem. Phys. 106 (1997) 9639.

[33] R. A. Kendall, T. H. Dunning Jr., R. J. Harrison, J. Chem. Phys. 96 (1992) 6796.

[34] L. Gyevi-Nagy, M. Kállay, P. R. Nagy, J. Chem. Theory Comput. 16 (2020) 366.

[35] G. Santra, J. M. L. Martin, J. Phys. Chem. A 126 (2022) 9375.

[36] G. Santra, E. Semidalas, N. Mehta, A. Karton, J. M. L. Martin, Phys. Chem. Chem. Phys. 24 (2022) 25555.

[37] E. Semidalas, J. M. L. Martin, J. Chem. Theory Comput. 18 (2022) 883.

[38] I. Efremenko, J. M. L. Martin, J. Phys. Chem. A 125 (2021) 8987. doi:10.1021/acs.jpca.1c05124.

[39] I. Sandler, S. Sharma, B. Chan, J. Ho, J. Phys. Chem. A 125 (2021) 9838.

[40] E. Paulechka, A. Kazakov, J. Chem. Theory Comput. 14 (2018) 5920.

[41] N. Sylvetsky, A. Banerjee, M. Alonso, J. M. L. Martin, J. Chem. Theory Comput. 16 (2020) 3641.

[42] A. Karton, B. Chan, Comput. Theor. Chem. 1217 (2022) 113874.

[43] Y. S. Al-Hamdani, P. R. Nagy, D. Barton, M. Kállay, J. G. Brandenburg, A. Tkatchenko, Nat. Commun. 12 (2021) 3927.

[44] N. C. Craig, P. Groner, D. C. McKean, J. Phys. Chem. A 110 (2006) 7461–7469.

[45] K. Kuchitsu, Structure Data of Free Polyatomic Molecules, volume 21, Springer-Verlag, Berlin,, 1992.

[46] J. Connett, J. Chem. Thermodyn. 4 (1972) 233–237.

[47] K. B. Wiberg, L. S. Crocker, K. M. Morgan, J. Am. Chem. Soc. 113 (1991) 3447–3450.

[48] M. Frisch, Chem. Phys. Lett. 166 (1990).

[49] G. W. Trucks, J. D. Watts, E. Salter, R. J. Bartlett, Chem. Phys. Lett. 153 (1988) 490–495.

[50] R. Krishnan, J. A. Pople, Int. J. Quantum Chem. 14 (1978) 91–100.